PERGAMON

Available online at www.sciencedirect.com
SCIENCE DIRECT®

Polyhedron 22 (2003) 2359–2362

POLYHEDRON

www.elsevier.com/locate/poly

Structures and magnetic properties of metal cubes

Masayuki Nihei [a], Norihisa Hoshino [b], Tasuku Ito [b], Hiroki Oshio [a,*]

[a] *Department of Chemistry, University of Tsukuba, Tennodai 1-1-1, Tsukuba 305-8571, Japan*
[b] *Department of Chemistry, Graduate School of Science, Tohoku University, Aoba-ku, Sendai 980-8578, Japan*

Received 8 October 2002; accepted 28 October 2002

Abstract

Structures and magnetic properties of copper(II), nickel(II) and manganese(II) cubes are presented. In the cubes, four metal ions are assembled into the cubes by tridentate Schiff base ligands. Magnetic succeptibility measurements revealed the copper and nickel cubes have high-spin ground state, while the manganese cube has a $S = 0$ spin ground state.

Keywords: Magnetic measurement; Shiff base; Cubane structure; Copper; Nickel; Manganese

---

1. Introduction

Multinuclear metal complexes with high-spin ground states have attached an intense interest due to the possibility of superparamagnetism. Such molecules show magnetic hysteresis [1] and quantum tunneling of magnetization [2–6], and the molecules are called as single molecule magnets [7–9]. The single molecule magnets need to have relatively high-spin ground state with a uniaxial magnetic anisotropy. On the other hand, transition metal complexes with a cubane structure have been very important class of compounds (M_4L_4) [10,11] where four metal ions are linked by hydroxo, alkoxo, azido, sulfido, or iminato bridges [12–14]. Magnetic properties of many alkoxo-bridged cubane complexes have been extensively studied, some of which have high-spin ground states [15–19]. It is, therefore, alkoxo-bridged cube can be a good candidate for construct high-spin molecules. Recently, we found Schiff base ligands can also be a bridging ligand to construct cubane core structures [20–23]. Here, we review structures and magnetic properties of tetranuclear copper(II), nickel(II) and manganese(II) cubes with Schiff base ligands, $[Cu_4(hsae)_4]\cdot 2H_2O\cdot 4CH_3CN$ (**1**), $[Ni_4(sae)_4(MeOH)_4]$ (**2**), and $[Mn^{II}_4(sap)_4(MeOH)_4]\cdot 2H_2O$ (**3**) (H_2hsae = 2-(4-hydroxysalicylideneamino)-1-ethanol, H_2sae = 2-salicylideneaminoethanol, and H_2sap = 2-salicylideneaminopropanol).

2. Experimental

2.1. Synthesis

All reagents were purchased and used without further purification. Schiff base ligands were prepared by condensation reactions of salicylaldehyde with the corresponding aminoalkylalcohol. The complexes were analyzed satisfactory as solvent-free. Complexes **1** and **2** were prepared in air, while the preparation of **3** was carried out under nitrogen atmosphere.

2.1.1. $[Cu_4(hsae)_4]\cdot 2H_2O\cdot 4CH_3CN$ (**1**)

H_2hsae (0.138 g, 1 mmol) was added to a solution of copper(II) acetate monohydrate (0.199 g, 1 mmol) in methanol (80 ml). A dark green powder was filtered, and recrystallization in acetonitrile gave dark blue tablets and one of them was subjected to the X-ray structural analysis. Elemental analysis: Found: (Calc.) C 45.25 (45.13), H 4.62 (4.48), N 9.40 (9.57).

2.1.2. $[Ni_4(sae)_4(MeOH)_4]$ (**2**)

H_2hsae (0.138 g, 1 mmol) was added to a solution of nickel(II) chloride hexahydrate (0.238 g, 1 mmol) in methanol (30 ml). After standing for 1 night, fine green

---

* Corresponding author. Tel./fax: +81-298-523-4238.
E-mail address: oshio@chem.tsukuba.ac.jp (H. Oshio).

0277-5387/03/$ - see front matter © 2003 Elsevier Science Ltd. All rights reserved.
doi:10.1016/S0277-5387(03)00159-1

crystals were precipitated. Recrystallization of the fine crystals from acetone and methanol gave green crystals suitable for X-ray structural analysis. Elemental analysis: Found: (Calc.) C 46.41 (46.48), H 5.27 (5.00), N 5.39 (5.23).

2.1.3. $[Mn^{II}_4(sap)_4(MeOH)_4]\cdot 2H_2O$ (**3**)

H_2hsap (0.152 g, 1 mmol) was added to a solution of manganese(II) chloride tetrahydrate (0.198 g, 1 mmol) in methanol (30 ml). After standing for several days, yellow crystals were precipitated suitable for X-ray structural analysis.

2.2. *Magnetic susceptibility measurements*

DC magnetic susceptibility data were collected by using a Quantum Design MPMS-5S SQUID magnetometer at temperatures ranging from 1.8 to 300 K.

3. Results and discussion

3.1. *Crystal structures of **1**–**3***

3.1.1. $[Cu_4(hsae)_4]\cdot 2H_2O\cdot 4CH_3CN$ (**1**)

The structure of **1** contains a tetranuclear cubane core (Fig. 1a), which locates on crystallographic twofold axis passing through the middle of Cu1···Cu1′ and Cu2···Cu2′ vectors, the asymmetric unit, thus, consists of the half of the tetramer. The cubane core consists of alkoxo bridged four copper atoms, giving an approximately cubic array of alternating copper and oxygen atoms. Intracluster metal–metal separations of Cu1···Cu2, Cu1···Cu1′, Cu1···Cu2′, and Cu2···Cu2′ pairs are 3.108(1), 3.443(1), 3.134(1), and 3.6154(9), respectively. Coordination geometry about each copper ion is a square pyramid with one nitrogen and two oxygen atoms from the ligand and two oxygen atoms from the next unit of the cubane. According to the bond lengths between the copper and coordinating atoms (i.e. four bonds with short bond distances (1.894(3)–2.000(3) Å) and bonds with long bond distances (2.467(3)–2.562(3) Å), basal planes for Cu1 and Cu2 are regarded as O1–N1–O2–O5′ and O4–N2–O5–O2 and the copper ions are displaced by 0.053(1) and 0.041(1) Å above the plane, respectively. The magnetic orbitals ($d_{x^2-y^2}$) of the Cu1 and Cu2 ions, which are perpendicular to each other, locate on the basal planes (Fig. 2a).

3.1.2. $[Ni_4(sae)_4(MeOH)_4]$ (**2**)

The structure of **2** is comprised of a tetranuclear cubane core, of which four nickel(II) ions were bridged by μ_3-alkoxo groups (Fig. 1b). A cubic array of

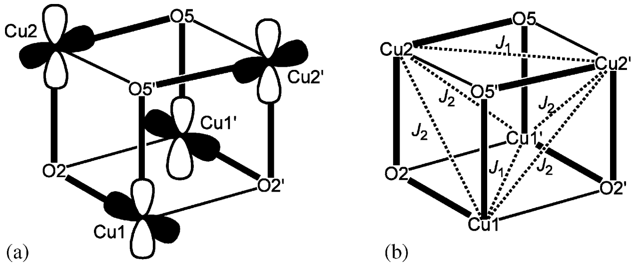

Fig. 2. Magnetic orbital arrangements (a) and exchange pass ways (b) of **1**. Thick lines represent bonds with short lengths.

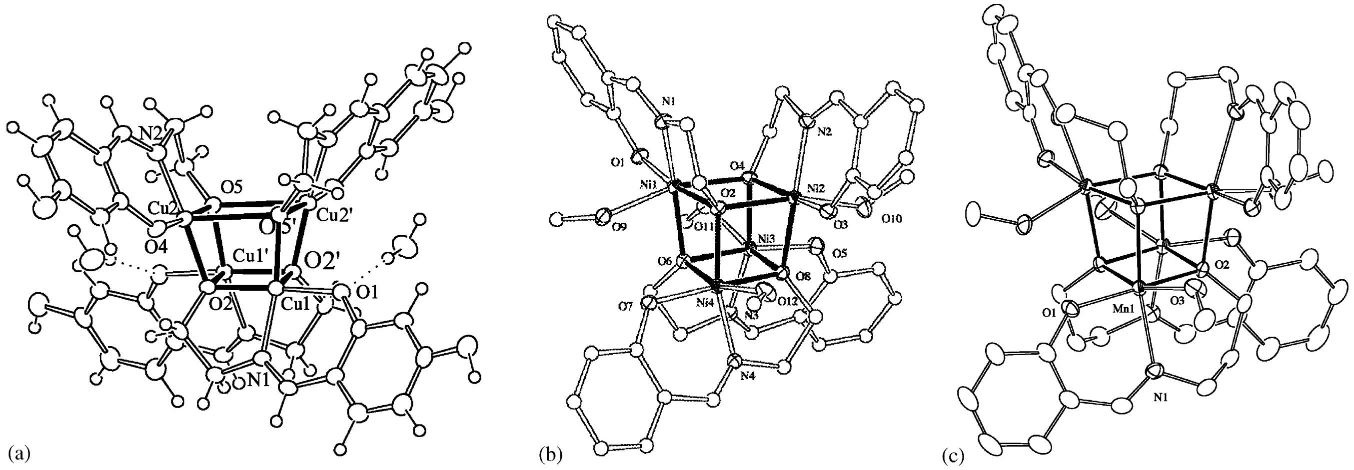

Fig. 1. ORTEP drawing of $[Cu_4(hsae)_4]\cdot 2H_2O\cdot 4CH_3CN$ (**1**) (a), $[Ni_4(sae)_4(MeOH)_4]$ (**2**) (b), and $[Mn^{II}_4(sap)_4(MeOH)_4]\cdot 2H_2O$ (**3**) (c). Selected distances [Å] and angles (°) with standard deviation in parentheses; **1**: Cu1–O1 1.894(3), Cu1–O2 1.959(3), Cu1–O2′ 2.467(3), Cu1–O5′ 1.956(3), Cu1–N1 1.925(4), Cu2–O2 1.930(3), Cu2–O4 1.939(3), Cu2–O5′ 2.562(3), Cu2–N2 1.914(4), Cu2–O5 2.000(3), Cu1–O2–Cu1′ 101.5(1), Cu1–O2–Cu2 106.1(1), Cu1′–O2–Cu2 90.1(1), Cu1–O5′–Cu2 85.8(1), Cu1–O5′–Cu2′ 104.8(1), Cu2–O5–Cu2′ 104.2(1). Symmetry operation (′): $1-x$, y, $3/2-z$. **2**: Ni(1)–O(2) 2.0218(19), Ni(1)–O(6) 2.0469(19) Ni(1)–O(4) 2.1207(18), Ni(2)–O(4) 2.0376(19), Ni(2)–O(8) 2.0522(19), Ni(2)–O(2) 2.1299(18), Ni(3)–O(4) 2.0331(19), Ni(3)–O(6) 2.0397(18), Ni(3)–O(8) 2.1197(19), Ni(4)–N(4) 1.989(2), Ni(4)–O(2) 2.0249(19), Ni(4)–O(8) 2.0257(18), Ni(4)–O(6) 2.1384(19). **3**: Mn(1)–O(1) 2.103(2), Mn(1)–O(2) 2.151 (2), Mn(1)–O(2)$^{\#1}$ 2.182(2), Mn(1)–N(1) 2.209(2), Mn(1)–O(2)$^{\#2}$ 2.233 (2), Mn(1)–O(3) 2.272(2). Symmetry operation: #1 $y-1/4$, $-x+1/4$, $-z+9/4$, and #2 $-x$, $-y+1/2$, z.

alternating nickel and oxygen atoms give intracluster metal–metal separations of 3.0347(5)–3.1981(5) Å. The coordination geometry about each nickel(II) ion is an axially elongated octahedron in which the equatorial sites are occupied by a tridentate sae^{2-} ligand and an alkoxo oxygen atom from the next unit of the cube. The coordination bond lengths with equatorial atoms are in the range of 1.976(2)–2.052(2) Å and a tetragonal elongation (2.120(2)–2.191(2) Å) occurs along the trans O–Ni–O bond vector involving methanol and bridging alkoxide. The bridging angles of the Ni–O–Ni bonds in the cube are in the range of 93.53(8)°–100.95(8)°.

*3.1.3. [$Mn_4^{II}(sap)_4(MeOH)_4$]·$2H_2O$ (**3**)*

Complex **3** crystallizes in tetragonal space group $I4_1/a$ and the asymmetric unit constructs quarter of cluster molecules in addition to solvent [7]. A complex molecule has S_4 symmetry and consists of a μ_3-alkoxo bridged tetranuclear core, giving an approximately cubic array of alternating manganese and oxygen atoms (Fig. 1c). Coordination geometry about each manganese(II) ion is a pseudo octahedron with one nitrogen and five oxygen atoms from tridentate sap^{2-} group and methanol molecule. Coordination bond lengths are 2.103(2)–2.272(2) Å for Mn–O and 2.209(2) Å for Mn–N, and the bridging bond angles of Mn–O(2)–Mn are in the range of 96.06(6)°–102.01(6)°. The Mn^{II} assignment for **2** is evident from the coordination geometry.

*3.2. Magnetic properties of **1–3***

Magnetic susceptibility measurements were performed on **1**, **2** and **3** in the temperature range of 1.8–300 K.

*3.2.1. [$Cu_4(hsae)_4$]·$2H_2O$·$4CH_3CN$ (**1**)*

The temperature dependence of the magnetic susceptibility of **1** was depicted in Fig. 3. At room temperature the value of χ_mT is 1.8 emu mol^{-1} K, which would be expected for non-correlated four spins. Upon cooling the χ_mT values increased until the maximum value of 2.44 emu mol^{-1} K at 14 K, then decreased. This magnetic behavior is indicative of an intracluster ferromagnetic interaction. The cubane unit has the twofold axis and the Jahn-Teller distortion elongates the axial bonds of Cu1–O2′ and Cu2–O5′, which leads to the weaken magnetic interaction between Cu2···Cu2′ and Cu1···Cu1′ pairs. The magnitude of magnetic interactions between Cu1···Cu2 and Cu1···Cu2′ pairs are considered to be comparable, because the structural analysis showed the similar bridging bond angles and lengths for the Cu1–O2–Cu2 (=106.1(1)°) and Cu1–O5′–Cu2′ (=104.8(1)°) bonds. The two exchange parameters J_1 and J_2 were, therefore, introduced for the analysis of the magnetic data (Fig. 2b). The experimental magnetic data were analyzed with the Hamiltonian operator $H = -2J_1\ (S_{Cu1}\cdot S_{Cu1'} + S_{Cu2}\cdot S_{Cu2'}) - 2J_2(S_{Cu1}\cdot S_{Cu2} + S_{Cu1}\cdot S_{Cu2'} + S_{Cu1'}\cdot S_{Cu2} + S_{Cu1'}\cdot S_{Cu2'})$ and the intercluster interaction was included as a mean field correction θ. The least squares calculation yielded the best fit parameters of g, J_1, J_2, and θ values being 2.02(1), $-17.6(1)$ cm^{-1}, $+36.0(9)$ cm^{-1} and $-1.0(1)$ K, respectively. The propagation of intracluster ferromagnetic interactions can be expected according to the known J versus bridging bond angles [24]. The magnetic orbital-overlap via oxygen p-orbitals becomes negligible for the bridging angles of Cu1–O2–Cu2 and Cu1–O5′–Cu2′ being 106.1(1)° and 104.8(1)°, respectively [25]. The perpendicular arrangement of the magnetic orbitals results in zero orbital overlap leading to the ferromagnetic interactions (J_2), while the parallel arrangement results in the antiferromagnetic interaction (J_1) (Fig. 2a).

*3.2.2. [$Ni_4(sae)_4(MeOH)_4$] (**2**)*

Temperature dependence of χ_mT values for **2** are displayed in Fig. 4. The room temperature χ_mT value (=4.99 emu mol^{-1} K) corresponds to the isolated four nickel(II) ions. Upon cooling, the χ_mT values increased to a maximum value of 8.76 emu mol^{-1} K at 8 K. This magnetic behavior is indicative of ferromagnetic interactions among the nickel(II) centers and predicts an $S =$

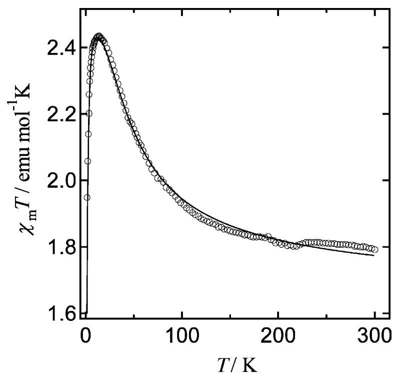

Fig. 3. Plots of χ_mT vs. T for 2^1. The solid line corresponds to the fit of the data as described in the text.

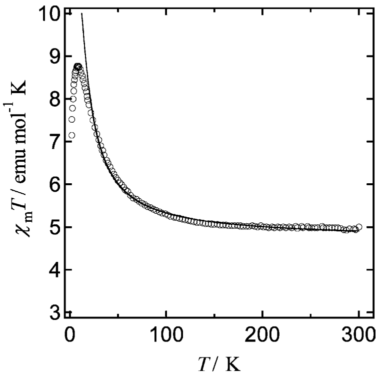

Fig. 4. Plot of χ_mT vs. T for 3^2. The solid line corresponds to the fit of the data as described in the text.

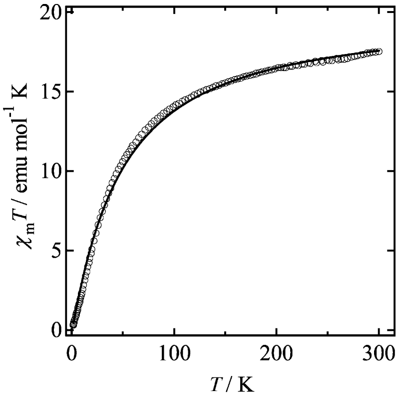

Fig. 5. Plots of $\chi_m T$ vs. T for **4**[3]. The solid line corresponds to the theoretical curves, parameters of which are given in the text.

4 spin ground state for **2**. A sudden decrease of the $\chi_m T$ values below 8 K is due to an inter-cube antiferromagnetic interaction and/or zero-field splitting. The magnetic data were analyzed by using Heisenberg spin Hamiltonian ($H = -2J\Sigma S_i \cdot S_j$) and the resulting expression of $\chi_m T$ was derived by the Kambe's method [26]. The least squares calculation yielded the best fit parameters of g and J values being 2.171 and 3.2 cm^{-1}, respectively.

3.2.3. $[Mn_4^{II}(sap)_4(MeOH)_4]\cdot 2H_2O$ (3)

The variable temperature magnetic susceptibility data for **3** show, on the other hand, the sign of antiferromagnetic interactions (Fig. 5). The $\chi_m T$ value of 17.57 emu mol^{-1} K at 300 K gradually decreases as the temperature is lowered, reaching to 0.29 emu mol^{-1} K at 2.0 K. The spin-only value for a unit composed of noninteracting Mn_4^{II} ions is 17.5 emu mol^{-1} K ($g = 2.0$). The temperature dependence of the $\chi_m T$ data was fitted in order to determine the magnitude of the antiferromagnetic coupling constant. Supposing the identical exchange coupling constants for intracube's magnetic pathways, the Kambe's vector coupling method [26] gives the eigenvalue expression as $E(S_T) = -J \cdot S_T \cdot (S_T + 1)(S_T = S_1 + S_2 + S_3 + S_4$ and $H = -2J\Sigma S_i \cdot S_j)$. The least squares calculation yielded the best fit parameters of g and J values being 2.141(1) and $-1.6(1)$ cm^{-1}, respectively. A manganese ion has d^5 electronic configuration, some of which magnetic orbitals direct to overlap each other. Therefore, the antiferromagnetic interaction overcomes the ferromagnetic interaction in the Mn cube.

4. Conclusion

Tridentate Schiff base ligands, prepared by the condensation reactions of salicylaldehyde and aminoalkylalchol give an opportunity to assemble a variety of four metal ions into cubes. Orthogonal arrangements for copper and nickel ions in the cube gave ferromagnetic interactions leading to high-spin ground states.

Acknowledgements

This work was partially supported by a Grant-in-aid for Scientific Researches from the Ministry of Education, Culture, Sports, Science and Technology, Japan.

References

[1] R. Sessoli, D. Gatteschi, A. Caneschi, M.A. Novak, Nature 365 (1993) 141.
[2] A.L. Barra, D. Gatteschi, R. Sessoli, Chem. Eur. J. 6 (2000) 1608.
[3] L. Thomas, F. Lionti, R. Ballou, D. Gatteschi, R. Sessoli, A.L. Barra, Nature 383 (1996) 145.
[4] J.R. Friedman, M.P. Sarachik, J. Tejada, R. Ziolo, Phys. Rev. Lett. 76 (1996) 3830.
[5] D. Gatteschi, A. Caneschi, L. Pardi, R. Sessoli, Science 265 (1994) 1054.
[6] A. Muller, F. Peters, M.T. Pope, D. Gatteschi, Chem. Rev. 98 (1998) 239.
[7] C. Boskovic, E.K. Brechin, W.E. Streib, K. Folting, J.C. Bollinger, D.N. Hendrickson, G. Christou, J. Am. Chem. Soc. 124 (2002) 3726.
[8] P. Artus, C. Boskovic, J. Yoo, W.E. Streib, L.-C. Brunel, D.N. Hendrickson, J. Christou, Inorg. Chem. 40 (2001) 4199.
[9] S.M.J. Aubin, M.W. Wemple, D.M. Adams, H.L. Tsai, G. Christou, D.N. Hendrickson, J. Am. Chem. Soc. 118 (1996) 7746.
[10] J.M. Berg, R.H. Holm, in: T.G. Spioro (Ed.), Iron-Sulfur Proteins, vol. 4 (Chapter 1), Wiley-Interscience, New York, 1982.
[11] R.H. Holm, S. Ciurli, J.A. Weigel, Prog. Inorg. Chem. 38 (1990) 1.
[12] M.A. Halcrow, J.C. Huffman, G. Christou, Angew. Chem., Int. Ed. Engl. 34 (1995) 889.
[13] M.A. Halcrow, J.S. Sun, J.C. Huffman, G. Christou, Inorg. Chem. 34 (1995) 4167.
[14] H.J. Mai, R.M. Köcker, S. Wocadlo, W. Massa, K. Dehnicke, Angew. Chem., Int. Ed. Engl. 34 (1995) 1235.
[15] L. Mertz, W. Haase, J. Chem. Soc., Dalton Trans. (1978) 1594.
[16] L. Schawabe, W. Haase, J. Chem. Soc., Dalton Trans. (1985) 1909.
[17] J.W. Hall, W.E.D. Estes, R.P. Scaringe, W.E. Williams, Inorg. Chem. 16 (1977) 1572.
[18] J. Sleten, A. Sorensen, M. Julve, Y. Journaux, Inorg. Chem. 29 (1990) 5054.
[19] J.A. Bertrand, A.P. Ginsberg, R.I. Kaplan, C.E. Kirkwood, R.L. Martin, R.C. Sherwood, Inorg. Chem. 10 (1971) 240.
[20] H. Oshio, N. Hoshiono, T. Ito, J. Am. Chem. Soc. 122 (2000) 12602.
[21] H. Oshio, Y. Saito, T. Ito, Angew. Chem., Int. Ed. Engl. 36 (1997) 267.
[22] N. Hoshino, T. Ito, M. Nihei, H. Oshio, Chem. Lett. (2002) 844.
[23] M. Nihei, N. Hoshino, T. Ito, H. Oshio, Chem. Lett. (2002) 1016.
[24] W.E. Hatfield, in: R.D. Willet, D. Gatteschi, O. Kahn (Eds.), Magneto-Structural Correlations in Exchange Coupled systems, NATO ASI Ser. C., vol. 140, 1985 p. 555.
[25] P.J. Hay, J.C. Thibeault, R. Hoffman, J. Am. Chem. Soc. 97 (1975) 4884.
[26] K. Kambe, J. Phys. Soc. Jpn 5 (1950) 48.